

Reactive Sulfur Species: Kinetics and Mechanism of the Oxidation of Aryl Sulfinates with Hypochlorous Acid

Hisanori Ueki, Garry Chapman, and Michael T. Ashby*

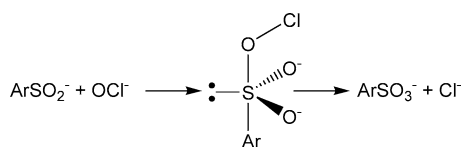
Department of Chemistry and Biochemistry, University of Oklahoma, Norman, Oklahoma 73019

Received: July 14, 2009; Revised Manuscript Received: October 30, 2009

The mechanism of oxidation of ArSO_2^- (PhSO_2^- and 5-sulfinato-2-nitrobenzoic acid = $\text{TNBO}_2^{1-/2-}$) with HOCl/OCl^- has been investigated using the kinetic method. In contrast to previous reports for PhSO_2^- (for which it was suggested that OCl^- and not HOCl was the reactant), the reaction proceeds through a conventional pathway: nucleophilic attack by ArSO_2^- on HOCl with concomitant Cl^+ transfer to give a sulfonyl chloride intermediate (ArSO_2Cl), which we have identified spectrophotometrically. Remarkably, the rate constant for the reaction of HOCl with ArSO_2^- is on the order of $10^9 \text{ M}^{-1} \text{ s}^{-1}$, larger than the rate constants for corresponding thiolates, and is nearly diffusion-controlled. In contrast, the rate constant for the reaction of OCl^- with ArSO_2^- is approximately 7 orders of magnitude smaller.

Introduction¹

Hypochlorous acid (HOCl) is considerably more reactive than its conjugate base, hypochlorite (OCl^-), usually by 4 or more orders of magnitude.² The most reactive partners with HOCl tend to have low oxidation potentials and be good nucleophiles.³ In general, the reactions proceed by electrophilic Cl^+ transfer. In some cases, the chlorinated species exhibit relative stability in water (e.g., for chloramines).⁴ However, subsequent hydrolysis often occurs rapidly in an aqueous environment to yield effective O-atom transfer, albeit vis-à-vis a stepwise mechanism that involves the aforementioned chlorinated intermediates. We are aware of only one mechanistic study with substantial evidence for faster oxidation by OCl^- versus HOCl : Kice and Puls reported in 1977 that OCl^- reacts with ArSO_2^- ($\text{Ar} = \text{Ph}$ and $p\text{-MeOC}_6\text{H}_4$) faster than HOCl reacts with ArSO_2^- to give ArSO_3^- .⁵ Based upon a pH-profile for the reaction (that suggested OCl^- , not HOCl , was the reactant), the stoichiometry, and the effects of Ar substituents, the authors suggested that OCl^- nucleophilically attacks ArSO_2^- to produce a sulfurane-like intermediate, which subsequently decomposes to give ArSO_3^- .⁵



Given the novel nature of the proposed pathway, we have reinvestigated the mechanism. We report here a detailed mechanistic study which evidence that the reactions of ArSO_2^- (PhSO_2^- and 5-sulfinato-2-nitrobenzoic acid = $\text{TNBO}_2^{1-/2-}$) with HOCl/OCl^- proceed via conventional pathways, with electrophilic Cl^+ transfer by HOCl to give sulfonyl chloride intermediates (ArSO_2Cl), which we have identified spectrophotometrically. We show that the kinetics of hydrolysis of PhSO_2Cl are consistent with the data that Kice and Puls attributed to the oxidation reaction. However, it is remarkable that the rates of

the reactions of aryl sulfinates with HOCl approach the diffusion limit, faster than the corresponding reactions of more nucleophilic thiolates.

Experimental Methods

General Details. All chemicals were ACS certified grade or better. Water was doubly distilled in glass. Solutions of NaOH , mostly free of CO_2 contamination, were quantified by titration with a standardized HCl solution using phenolphthalein as an indicator. HClO_4 solution was standardized against bicarbonate. Electronic spectra were measured using a HP 8452A diode array spectrophotometer or the monochromator of a HI-TECH SF-61 DX2 stopped-flow instrument. For fast reactions, kinetic measurements were made with a HI-TECH stopped-flow spectrophotometer using a Xe arc lamp and PMT detector. During the stopped-flow measurements, the temperature was maintained at 291 K with a Lauda RC-20 circulator. The adiabatic temperature increases that were associated with the pH jump experiments were determined experimentally to be less than 1 °C. For slow reactions, kinetic data were measured with the diode-array instrument. The pH values of the buffered solutions were determined with an Orion Ion Analyzer EA920 using an Ag/AgCl combination pH electrode. Unless otherwise noted, all kinetic measurements were made using solutions for which the ionic strengths had been adjusted to 1.0 using NaClO_4 .

Materials. $\text{PhSO}_2^- \cdot \text{Na}^+$ (98%, Aldrich), PhSO_2Cl (99%, Aldrich), and PhSO_3H (>98%, Fluka) were used as received from the manufacturers. An improved synthesis of 5-mercapto-2-nitrobenzoic acid (TNB) from 5,5'-dithiobis(2-nitrobenzoate) (DTNB or Ellman's reagent), as well as the first syntheses of 5-sulfino-2-nitrobenzoic acid (TNBO_2), 5-sulfo-2-nitrobenzoic acid (TNBO_3), and 3-carboxy-4-nitrobenzenesulfonyl chloride (TNBO_2Cl) will be described elsewhere. All of the new compounds that were employed in this study were fully characterized by ^1H NMR, ^{13}C NMR, HRMS, and UV–visible spectroscopy. The UV–visible spectra of the TNB derivatives are generally unique (Table 1).

HPLC Analysis of DTNB, TNB, TNBO_2 , TNBO_3 , and TNBO_2Cl . HPLC analysis was performed using conditions similar to those employed previously.⁶ A Zorbax SB C18 column (4.6 × 150 mm, 5 μm) was used for all analyses. The

* Corresponding author. E-mail: MAshby@ou.edu.

TABLE 1: Molar Absorption Coefficients in Aqueous Media

compound	solution (pH)	λ_{\max} (nm)	ϵ_{\max} ($M^{-1}\cdot\text{cm}^{-1}$)
DTNB ²⁻	PBS (7.4)	324	16330
DTNB ⁰	HClO ₄ (0.0)	316	9800
TNB ²⁻	PBS (7.1)	412	14150
TNB ⁰	HClO ₄ (0.0)	330	9140
TNBO ₂ ²⁻	PBS (7.2)	268	5760
TNBO ₃ ²⁻	PBS (7.2)	264	5800
TNBO ₂ Cl ⁰	HCl (0.0)	234	~7500 ^a
PhSO ₂ ⁻	NaOH (14.0)	264	950
PhSO ₃ ⁻	NaOH (14.0)	262	380
PhSO ₂ Cl ⁰	HClO ₄ (1.0)	234	>6500 ^a

^a The accuracy of ϵ is affected by hydrolysis.

flow rate of eluent (45% CH₃CN/55% H₂O, 0.1% TFA) was set at 1.5 mL/min for the analyses of DTNB, TNB, and TNBO₂Cl. The retention times were 19.8, 11.2, and 16.1 min, respectively. For TNBO₂ and TNBO₃, a more polar eluent (5% CH₃CN/95% H₂O, 0.1% TFA) was used, and the flow rate was set at 1.0 mL/min. The retention times were 16.5 and 10.7 min, respectively.

Kinetic Study of the Oxidation of PhSO₂⁻ with HOCl/OCl⁻. The oxidation was investigated using conditions that were comparable to those employed by Kice and Puls.⁵ Stock solutions of PhSO₂⁻ were prepared by dissolving a known amount of the sulfinic acid in phosphate buffer. HOCl/OCl⁻ solutions were prepared by diluting standardized aqueous solutions of NaOCl in phosphate buffer. The sulfinate solution was mixed with freshly prepared solutions of HOCl/OCl⁻ in a 1/1 ratio using a hand-mixer to give [PhSO₂Na] = 0.35 mM and [NaOCl] + [HOCl] = 2.13 mM. The pH value after mixing was 6.01. The reaction was monitored with a diode-array instrument.

Kinetic Study of the Hydrolysis of TNBO₂Cl. The solubility of TNBO₂Cl in aqueous base is relatively high, although it hydrolyzes quickly. Conversely, TNBO₂Cl hydrolyzes more slowly in aqueous acid, but it exhibits poor solubility therein. On the basis of these restrictions, two experimental methods were designed for measuring the hydrolysis of TNBO₂Cl.

Method A (for slow reactions at pH 0–8): A known amount of TNBO₂Cl was dissolved in 1 mL of dioxane. An aliquot was diluted 100 times with aqueous buffer (phosphate buffer for pH 1.89–3.05 and 5.79–8.15; acetate buffer for pH 3.82–5.27) or nonbuffered (pH 0–1) solutions. Immediately thereafter, the hydrolysis reaction was monitored using a diode-array instrument.

Method B (for fast reactions at pH 10.6–14): A known amount of TNBO₂Cl was dissolved in 1 mL of dioxane. An aliquot was diluted 100 times with 0.5 M HClO₄. The freshly prepared TNBO₂Cl solution in 0.5 M HClO₄ and 1% dioxane solution was placed in a reservoir syringe of the stopped-flow instrument. Buffered (phosphate buffer for pH 10.61–12.11) or nonbuffered (pH > 11) solutions containing 0.5 M NaOH were placed in another reservoir syringe of the stopped flow instrument. The hydrolysis was measured in single-mixing mode with the HI-TECH stopped-flow spectrophotometer.

Kinetic Study of the Hydrolysis of TNBO₂Cl in the Presence of HOCl/OCl⁻. Using a hand-mixer, a freshly prepared TNBO₂Cl solution in 0.5 M HClO₄ with 1% dioxane was mixed in 1:1 ratio with a freshly prepared HOCl/OCl⁻ phosphate-containing solution containing 0.5 M NaOH. Then, the reaction was monitored with a diode-array instrument.

Kinetic Study of the Oxidation of TNBO₂ with HOCl/OCl⁻. TNBO₂ is soluble and relatively stable in aqueous media regardless of the pH. However, TNBO₂ is slowly oxidized by O₂ in aqueous solutions to give TNBO₃. HOCl/OCl⁻ decom-

poses relatively quickly under neutral⁷ to acidic conditions,⁸ whereas OCl⁻ is relatively stable under strong basic conditions. The following experiment was designed on the basis of these chemical properties. Using a hand-mixer or the HI-TECH instrument, a solution containing 200 μ M TNBO₂Na₂, 0.1 M HClO₄ and buffer (none for pH 1, 13, and 14; phosphate buffer for pH 2–3, 5.81–8.2, and 10.14–12.31; acetate buffer for pH 3.91–5.1) was mixed in a 1:1 ratio with a NaOCl solution in 0.1 M NaOH. The ensuing reaction was monitored with a diode array instrument or with the spectrophotometer of the HI-TECH stopped-flow instrument.

General Data Analysis. Monochromatic kinetic traces were modeled by single- or double-exponential equations using KaleidaGraph 3.6 (Synergy Software). The concentration dependencies of the pseudo-first-order rate constants were obtained by linear least-squares fits. Polychromatic data were analyzed using SPECFIT/32 (Spectrum Software Associates), a multi-variate data analysis program.

Calibration of the HI-TECH SF-61 DX2 Stopped-Flow Instrument and Analysis of the Data of Figure 6. Measurement of the kinetic trace of Figure 6 required additional precautions. The instrument was calibrated using the reaction of 2,6-dichlorophenol–indophenol (DCIP) and ascorbic acid (AA) at pH = 1.80 under pseudo-first-order conditions (excess [AA]).⁹ The plot of [AA] vs k_{obs} started to deviate from linearity when k_{obs} was larger than 400 s⁻¹, indicating that the highest limit of k_{obs} that could be measured for a (pseudo-)first-order reaction on our HI-TECH SF-61 DX2 stopped-flow instrument is 400 s⁻¹. The dead time and the pretriggering time of the instrument were determined on the basis of the following equations:

$$\text{Deadtime: } A_{\text{obs}} = A_{\text{tot}} e^{-k_{\text{obs}} t_d}$$

$$\text{Pre-triggering time: } A_{\text{tot}} = A_{\text{fit}} e^{-k_{\text{obs}} t_s}$$

where A_{obs} is the observed absorbance maximum; A_{tot} is the effective absorbance change associated with the reaction; A_{fit} is the fitted absorbance change (extrapolated to $t = 0$); t_d is the dead time and t_s is the pretriggering time of the instrument. It has been previously shown mathematically that it should be necessary to correct for a concentration gradient within the stopped-flow observation cell for fast second-order reactions, where the aging of the reaction mixture has to be taken into account and the observed rate constants have to be corrected using the geometrical parameters of the observation cell).¹⁰ The half-life for the reaction of Figure 6 is ca. 6 ms, close to the mixing time of the instrument. However, as has been observed previously,¹⁰ standard second-order treatment (which ignores the existence of a concentration gradient) yielded a rate constant that was statistically identical to one computed when the gradient was taken into account. Furthermore, we investigated the effect of the mixing rate constant (k_{mix}) on k_{obs} and we have found that no correction was necessary for the data collected with our instrument for the reaction conditions of Figure 6.

Results

Products of the Reaction of HOCl/OCl⁻ with ArSO₂⁻ and Hydrolysis of ArSO₂Cl. The eventual products of the oxidation of ArSO₂⁻ (PhSO₂⁻ and TNBO₂¹⁻²⁻) with HOCl/OCl⁻ in aqueous medium were the ArSO₃⁻ derivatives. The ArSO₃⁻ derivatives were also observed as the only organic products of the hydrolysis

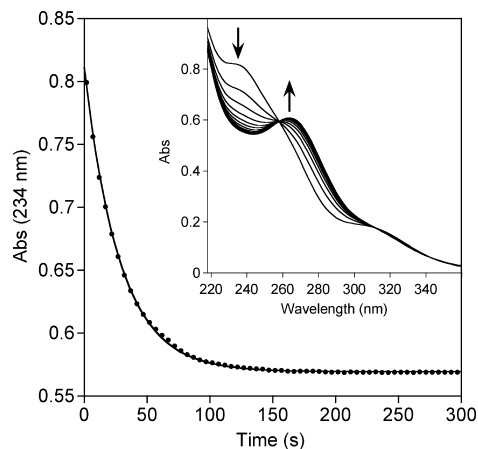


Figure 1. Absorbance decrease at 234 nm (λ_{\max} for TNBO_2Cl) observed when TNBO_2 ($100 \mu\text{M}$) is reacted with NaOCl ($100 \mu\text{M}$) in 0.3 M PBS at $\text{pH} = 7.29$ and $I = 1.0 \text{ M}$ (PBS + NaClO_4). Twenty percent of the data are illustrated (for clarity) with a first-order fit ($k = 0.0355 \pm 0.0001 \text{ s}^{-1}$). Inset: UV-vis spectra recorded at 1 s intervals (data for 12 s intervals illustrated for clarity). SVD modeling of these data with a first-order model yielded $k = 0.0358 \pm 0.0001 \text{ s}^{-1}$.

of ArSO_2Cl . The ArSO_3^- products were identified by ^1H NMR, HPLC, and UV-vis using authentic samples (data not shown).

Characterization of an Intermediate Observed During the Reaction of HOCl/OCl^- with ArSO_2^- . ArSO_2Cl (PhSO_2Cl and TNBO_2Cl) were observed spectrophotometrically as intermediates during the reaction of ArSO_2^- with HOCl/OCl^- . The sulfonyl chlorides were identified by their unique UV-vis spectra using authentic samples (Table 1). Figure 1 illustrates a typical time-resolved experiment for the reaction of TNBO_2^{2-} ($100 \mu\text{M}$) with HOCl/OCl^- ($100 \mu\text{M}$) at $\text{pH} 7.3$. Note that $\lambda_{\max} = 268 \text{ nm}$ for TNBO_2^{2-} , but the first spectrum that is observed (Figure 1, inset) exhibits an absorbance maximum at 234 nm, which is characteristic of TNBO_2Cl (Table 1). During the time interval of 300 s, the spectrum of TNBO_2Cl is replaced with the spectrum for TNBO_3^{2-} (with a $\lambda_{\max} = 264 \text{ nm}$). A similar observation was made when PhSO_2^- ($\lambda_{\max} = 262 \text{ nm}$) was oxidized with HOCl/OCl^- to give PhSO_3^- ($\lambda_{\max} = 264 \text{ nm}$) vis-à-vis PhSO_2Cl ($\lambda_{\max} = 234 \text{ nm}$).

Kinetics of the Hydrolysis of ArSO_2Cl . Given the observation of ArSO_2Cl as an intermediate (vide supra), in preparation for measuring the rates of oxidation, we investigated the hydrolysis of ArSO_2Cl (PhSO_2Cl and TNBO_2Cl). The rate of hydrolysis of TNBO_2Cl was studied between $\text{pH} 0$ and 13.7. At all values of pH , a decrease in the absorbance at 234 nm (λ_{\max} for TNBO_2Cl) was observed with a proportional increase in the absorbance at 264 nm (λ_{\max} for TNBO_3). All of the kinetic traces were described by single exponential equations, which indicate that the reaction proceeds with pseudo-first-order kinetics with a first-order dependence upon $[\text{TNBO}_2\text{Cl}]_0$. Figure 2 illustrates that the rate of oxidation for $[\text{TNBO}_2]_0 = [\text{HOCl}]_0 + [\text{OCl}^-]_0 = 100 \mu\text{M}$ is identical to the rate of hydrolysis of TNBO_2Cl for the approximate pH range that was investigated by Kice and Puls.⁵ For each pH , TNBO_2Cl was observed as the primary TNB derivative (as identified by $\lambda_{\max} = 234 \text{ nm}$) in the first spectrum that was collected. Similar data were collected for the reaction of PhSO_2^- with HOCl/OCl^- under the same conditions employed by Kice and Puls, and PhSO_2Cl was the first observable species (data not shown). The rate of hydrolysis of TNBO_2Cl^- was also investigated between $\text{pH} 10$ and 14 in unbuffered medium. No change in pH was observed for these reactions (because $[\text{OH}^-]$ was in large excess with respect to $[\text{TNBO}_2\text{Cl}]_0$). The pseudo-first-order rate constants

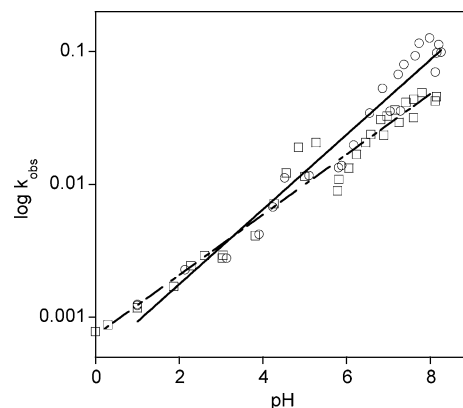


Figure 2. Log-log plot of k_{obs} (s^{-1}) vs $[\text{H}^+]$ for the oxidation (circles, with exponential fit illustrated with a solid line) of TNBO_2 ($100 \mu\text{M}$) with NaOCl ($100 \mu\text{M}$) and hydrolysis (squares, with exponential fit illustrated with a dashed line) of TNBO_2Cl ($88.5\text{--}117 \mu\text{M}$) for $0 \leq \text{pH} \leq 8.3$. All the data sets were fitted to a first-order rate law with SVD analysis of the entire UV-vis spectra. Buffer = (none, phosphate, or acetate) and $I = 1.0 \text{ M}$ (buffer + NaClO_4).

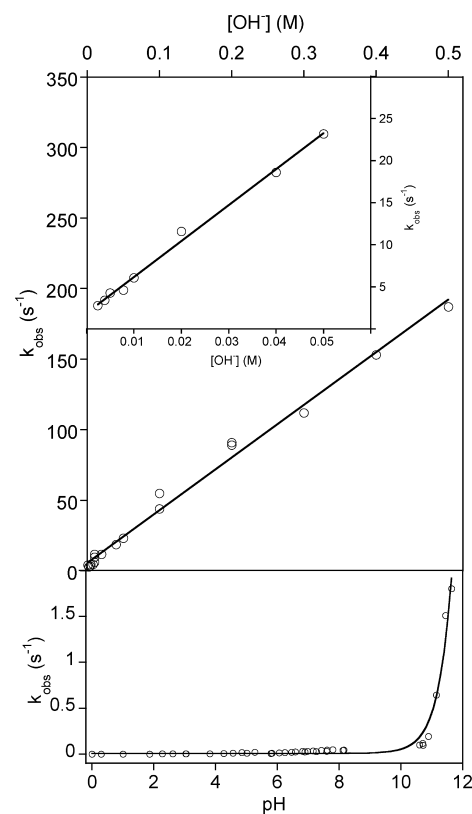


Figure 3. Top: effect of $[\text{OH}^-]$ on the hydrolysis of TNBO_2Cl in unbuffered solution. The inset is an expansion of the same data. All the data sets are well fitted to a first-order rate law with SVD analysis of the entire UV-vis spectra. Based on the slope and intercept of the linear fits (illustrated), $k_0 = 5.5123 \text{ [s}^{-1}\text{]}$ and $k_{\text{OH}} = 373.48 \text{ [M}^{-1} \text{ s}^{-1}\text{]}$. Conditions: $[\text{TNBO}_2\text{Cl}]_0 = 96 \mu\text{M}$, 1% dioxane, $I = 1.0 \text{ M}$ ($\text{NaOH} + \text{NaClO}_4$). Bottom: $\text{pH}-k_{\text{obs}}$ profile for the hydrolysis of TNBO_2Cl in the 0–12 pH range. All time traces were fit to first-order rate laws with SVD analysis of the entire UV-vis spectra. Conditions: $88.5\text{--}117 \mu\text{M}$ TNBO_2Cl , 0.3 M buffer (none, phosphate, or acetate for $\text{pH} 0\text{--}12$), 0.5–1% dioxane, $I = 1.0 \text{ M}$ (buffer + NaClO_4). Based on a fit of the entire data set to the equation $k_{\text{obs}} = k_0 + k_{\text{OH}}[\text{OH}^-]$ (illustrated), $k_0 = 0.008 \pm 0.011 \text{ s}^{-1}$ and $k_{\text{OH}} = 438 \pm 13 \text{ M}^{-1} \text{ s}^{-1}$.

were determined by SVD analysis of polychromatic data. The combined data sets are summarized in Figure 3. The rate of hydrolysis of PhSO_2Cl has been investigated previously,¹¹ albeit not above $\text{pH} 11$, and not for $I = 1$. For the purpose of the

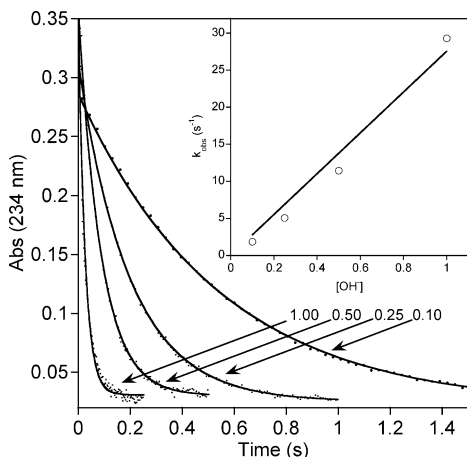


Figure 4. Effect of $[\text{OH}^-]$ on the rate of hydrolysis of PhSO_2Cl ($50 \mu\text{M}$). Conditions: $50 \mu\text{M}$ PhSO_2Cl , unbuffered, 0.5% dioxane, $I = 1.0 \text{ M}$ ($\text{NaOH} + \text{NaClO}_4$). First-order fits are illustrated (20% of the data shown). Inset: relationship between k_{obs} (s^{-1}) and $[\text{OH}^-]$, fit with a linear function to give $k_{\text{OH}} = 27 \pm 1 \text{ M}^{-1} \text{ s}^{-1}$.

present study (vide infra), it was necessary to measure the rate of hydrolysis of PhSO_2Cl for pH 13–14 and $I = 1$ (Figure 4).

Kinetics of the Reaction of ArSO_2^- with HOCl/OCl^- . The rate of reaction of ArSO_2^- with HOCl/OCl^- exceeds the capabilities of the stopped-flow method below pH 9. The rate of hydrolysis of TNBO_2Cl^- becomes faster than the rate of oxidation of TNBO_2^{2-} above pH 12. However, over the narrow pH range of 10.5–11.5 when $[\text{TNBO}_2^{2-}]_0 = [\text{OCl}^-]_0$ (an excess of one or the other would accelerate the oxidation reaction rate), we observe both reactions. Figure 5 illustrates kinetic traces for the reaction of TNBO_2^{2-} ($100 \mu\text{M}$) with OCl^- ($100 \mu\text{M}$) at pH 10.5, as monitored at two wavelengths: 230 nm (near λ_{max} for TNBO_2Cl^-) and 260 nm (near λ_{max} of TNBO_3^{2-}). Note that Kice and Puls employed higher reactant concentrations ($[\text{PhSO}_2^-]_0 = 300\text{--}600 \mu\text{M}$ and $[\text{HOCl}]_0 + [\text{OCl}^-]_0 = 2\text{--}3 \text{ mM}$) and lower pH (5–9) than the conditions we employed to collect the data of Figure 5. The traces of Figure 5 exhibit biphasic kinetics, as expected for a stepwise reaction (Table 2). The upper trace of Figure 5 for 230 nm (λ_{max} for TNBO_2Cl^- is 234 nm) exhibits an initial increase in absorption, followed by a decrease, as expected for the formation of an intermediate, TNBO_2Cl^- , that subsequently hydrolyzes to give TNBO_3^{2-} . As expected, the lower trace at 260 nm (λ_{max} for TNBO_3^{2-} is 264 nm) mirrors this behavior, with an initial decrease in absorption, followed by an increase in absorption (as expected for an initial decrease in $[\text{TNBO}_2^{2-}]$ followed by the formation of TNBO_3^{2-}). At lower pH, only the second reaction is observed (vide infra).

Reaction Conditions Where Oxidation Is Faster Than Hydrolysis. The rate of oxidation of ArSO_2^- by HOCl can only be monitored over a very narrow pH range of ca. 9.0–9.5 (at very low reactant concentrations) and above pH 13. The oxidation reaction is too fast to monitor using the stopped-flow method below pH 9 (for concentrations of reactants that produce sufficient changes in absorption). Between pH 10 and 13, the rate of hydrolysis is competitive with the rate of oxidation (e.g., Figure 5). Above pH 13, oxidation can become rate-limiting (if the reactant concentrations are sufficiently high). Since we were interested in extrapolating to the pH range that was studied by Kice and Puls (pH 5–9), we investigated the rate of reaction of PhSO_2^- with OCl^- at pH 9. One of the few buffer systems that is effective near pH 9 is borate. Unfortunately, we have observed that sulfonyl chlorides react with the borate buffer (unpublished results). However, this is not problematic for

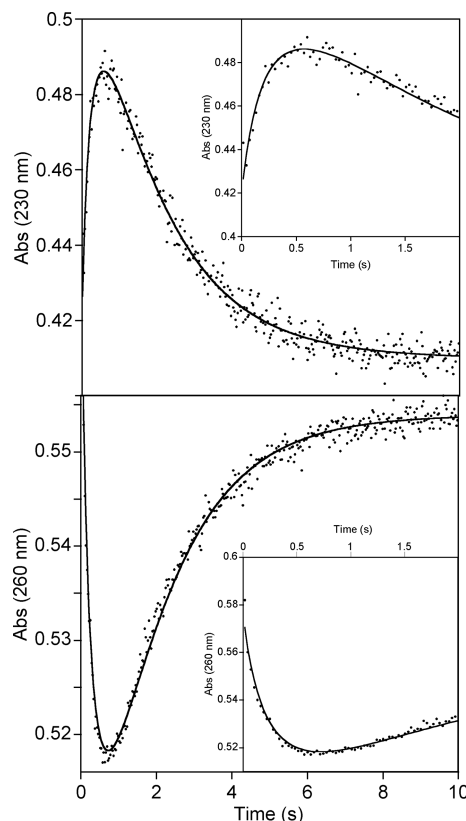


Figure 5. Biphasic absorption changes that occur at 230 nm (λ_{max} for TNBO_2Cl^- is 234 nm) and at 260 nm (λ_{max} for TNBO_2 and TNBO_3 are 268 and 264 nm, respectively), observed when TNBO_2 ($100 \mu\text{M}$) is reacted with NaOCl ($100 \mu\text{M}$) in 0.3 M PBS at pH = 10.5 and $I = 1.0 \text{ M}$ (PBS + NaClO_4). A fit using the model $\text{A} + \text{B} \rightarrow \text{C} \rightarrow \text{D}$ is illustrated. The insets are the same data with expanded abscissa axes.

TABLE 2: SVD Analyses of the Polychromatic Data That Exhibit Biphasic Kinetics between pH 10 and 11.5 for the Oxidation of TNBO_2^{2-} ($100 \mu\text{M}$) by NaOCl ($100 \mu\text{M}$) Using the Model $\text{A} + \text{B} \rightarrow \text{C} \rightarrow \text{D}^a$

pH	k_{obs} ($\text{M}^{-1} \text{ s}^{-1}$) ^b $\times 10^{-4}$	k'_{obs} (s^{-1}) ^b	k_{HOCl} ($\text{M}^{-1} \text{ s}^{-1}$) ^c $\times 10^8$
10.14	59.4 ± 0.7	0.1414 ± 0.0004	3.2 ± 0.3
10.47 ^b	18.5 ± 0.4	0.2323 ± 0.0006	2.18 ± 0.02
10.77	10.3 ± 0.1	0.2391 ± 0.0007	2.43 ± 0.01
10.84	5.76 ± 0.08	0.377 ± 0.001	1.17 ± 0.02
11.01	4.15 ± 0.06	0.462 ± 0.002	1.7 ± 0.1
11.29	3.77 ± 0.07	0.660 ± 0.005	2.92 ± 0.06
11.5	1.05 ± 0.02	0.93 ± 0.01	3.32 ± 0.09
			$X = 2.4 \pm 0.8$

^a Two traces of this data set are illustrated in Figure 5. ^b k_{obs} = the rate constants for the formation of TNBO_2Cl^- and k'_{obs} = the rate constants for the hydrolysis of TNBO_2Cl^- . ^c $k_{\text{HOCl}} = k_{\text{obs}} K_a^{\text{HOCl}} / [\text{H}^+]$.

investigating the first reaction, oxidation of ArSO_2^- with OCl^- , because the subsequent reaction of ArSO_2Cl with borate is relatively slow at pH 9. The reaction for $[\text{PhSO}_2^-]_0 = [\text{OCl}^-]_0 = 25 \mu\text{M}$ at pH 9 is illustrated in Figure 6. Equimolar reaction conditions were chosen to minimize the reaction rate (of the hetero-second-order reaction) while employing the minimum concentration that yielded sufficient absorbance change to accurately determine the rate. The final absorption (0.065 au) corresponds to the absorption at 234 nm of the (transient) spectrum of PhSO_2Cl (Figure 6, inset). The difference in absorption between the starting PhSO_2^- reactant and the PhSO_2Cl ($\Delta\text{Abs}_{234\text{nm}} = 0.065 - 0.010 = 0.054 \text{ au}$), as well as

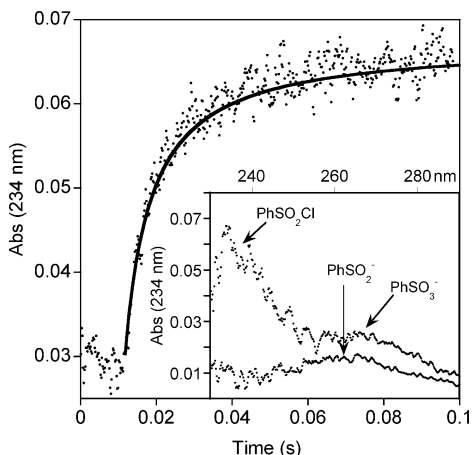


Figure 6. Absorption change that occurs at 234 nm (λ_{max} for PhSO_2Cl) that is observed (an average of 20 mixing cycles) when PhSO_2^- (25 μM) is reacted with NaOCl (25 μM) in 50 mM borate buffer at $\text{pH} = 9.0$ and $I = 1.0$ M ($\text{NaH}_2\text{BO}_3 + \text{NaClO}_4$). A hetero-second-order fit is illustrated ($k_{\text{obs}} = 2.32(9) \times 10^7 \text{ M}^{-1} \text{ s}^{-1}$). Inset: the absorption spectrum of 25 mM PhSO_2^- and 1 min after reaction with 25 mM NaOCl .

the change that is observed in the time trace ($\Delta\text{Abs}_{234\text{nm}} = 0.065 - 0.030 = 0.035$ au), suggests that ca. 45% of the reaction has occurred in the mixing time of the stopped-flow experiment. This was taken into consideration when fitting the data set of Figure 6 to a second-order rate function.

Reaction Conditions Where Oxidation Is Competitive with (or Slower Than) Hydrolysis. The data of Figure 5 (and related conditions) illustrate both the oxidation and hydrolysis reactions. However, it is difficult to accurately measure the rate of oxidation under such conditions because the oxidation reaction remains fast, and because it overlaps with the hydrolysis reaction from $\text{pH} 10$ – 13 . Ideally, the $[\text{OCl}^-]$ would be raised to the point that its disappearance could be measured directly ($\epsilon_{292\text{nm}}(\text{OCl}^-) = 350 \text{ M}^{-1} \text{ cm}^{-1}$). This is not possible below $\text{pH} 13$, as the reaction becomes too fast to measure by stopped-flow. However, it is possible to make such measurements above $\text{pH} 13$ (Figure 7). The data of Figure 7 that were collected at 234 nm (λ_{max} for PhSO_2Cl , cf. the analogous data for TNBO_2Cl of Figure 5) illustrate the biphasic kinetics that we interpret as the formation of PhSO_2Cl and its subsequent hydrolysis (vide supra). More PhSO_2Cl is produced at $[\text{OH}^-] = 0.1$ M than at $[\text{OH}^-] = 1.0$ M, as expected for faster oxidation (vide infra) and slower hydrolysis at lower pH. In contrast to the kinetic traces at 234 nm, the kinetic traces at 292 nm (λ_{max} for OCl^-) exhibit simple first-order behavior. Thus, the ΔAbs at 292 nm is proportional to $-d[\text{OCl}^-]/dt$ and the rate of the oxidation reaction. The data of Figure 7 were collected under the pseudo-first-order reaction conditions $[\text{PhSO}_2^-]_0 = 100 \mu\text{M}$ and $[\text{OCl}^-]_0 = 1 \text{ mM}$ (although an analogous set of data were also collected for $[\text{PhSO}_2^-]_0 = 1 \text{ mM}$ and $[\text{OCl}^-]_0 = 100 \mu\text{M}$, data not shown). The kinetic traces at 292 nm are well-described by a first-order model (Figure 7, top). The values of k_{obs} (s^{-1}) that were determined at 292 nm are plotted versus $1/[\text{OH}^-]$ in the inset of Figure 7. The significance of the slope and intercept of the line that describes the data will be discussed later. We attribute the pH dependence to the reaction of HOCl (not OCl^-), even at the very high pH of Figure 7 ($\text{pH} 13$ – 14). The reason for the dominance of HOCl at $\text{pH} 13$ – 14 (5.6–6.6 orders of magnitude from the $\text{p}K_{\text{a}}$ of HOCl) is the fact that k_{HOCl} is near the diffusion limit (10^9 – $10^{10} \text{ M}^{-1} \text{ s}^{-1}$) and is about 7 orders of magnitude greater than k_{OCl^-} (vide infra). The biphasic data of Figure 7 were fit to a double exponential function that describes

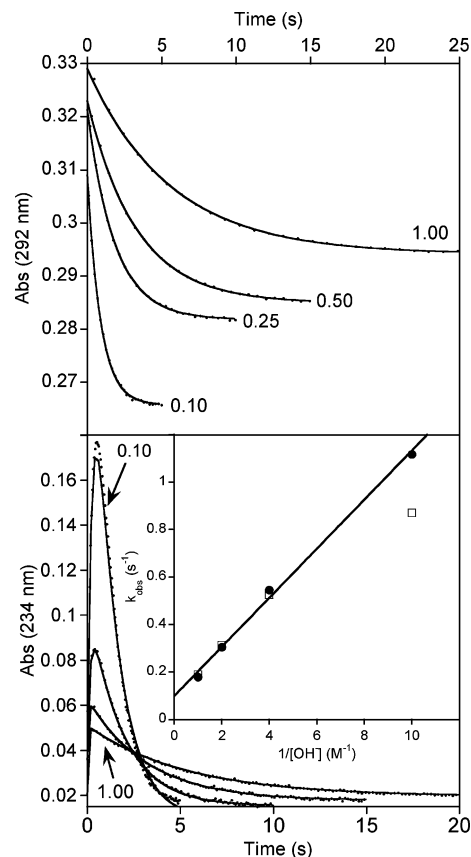


Figure 7. Top: absorption change that occurs at 292 nm (λ_{max} for OCl^-) that is observed when PhSO_2^- (1 mM) is reacted with NaOCl (1 mM) in unbuffered medium with $0.1 \leq [\text{OH}^-] \leq 1.0$ M and $I = 1.0$ M ($\text{NaOH} + \text{NaClO}_4$). First-order fits are illustrated (5% of the data shown). Bottom: absorption change at 234 nm (λ_{max} for PhSO_2Cl) that occurs under the same reaction conditions. Double exponential fits are illustrated (20% of the data shown). Inset: plot of k_{obs} computed from both sets of data that corresponds to the oxidation reaction versus $1/[\text{OH}^-]$ (circles are for $\lambda = 292$ nm and squares are for $\lambda = 234$ nm). These rate data are summarized in Table 3. All of the data points were included in the linear fit except for the square that lies off the line (which corresponds to $\lambda = 234$ nm when the rate of hydrolysis is comparable to the rate of oxidation).

TABLE 3: Comparison of the Pseudo-First-Order Rate Constants for Hydrolysis (k_{hyd}) and Oxidation (k_{ox}) as a Function of $[\text{OH}^-]$

$[\text{OH}^-]$	$k_{\text{hyd}} (\text{s}^{-1})^a$	$k_{\text{hyd}} (\text{s}^{-1})^b$	$k_{\text{ox}} (\text{s}^{-1})^c$	$k_{\text{ox}} (\text{s}^{-1})^b$
0.10	1.84 ± 0.01	3.63 ± 0.07	1.117 ± 0.003	0.87 ± 0.01
0.25	5.07 ± 0.02	6.50 ± 0.07	0.545 ± 0.003	0.525 ± 0.005
0.50	11.43 ± 0.05	17.3 ± 0.6	0.304 ± 0.001	0.313 ± 0.001
1.00	29.3 ± 0.2	30 ± 1	0.179 ± 0.001	0.1884 ± 0.0009

^a Measured directly using PhSO_2Cl and pH ump (Figure 4).

^b Deconvoluted from the biphasic data of Figure 7 (bottom).

^c Measured directly at $\lambda = 292$ (Figure 7, top).

sequential (pseudo-)first-order reactions. In general, when the two rate constants (k_1 and k_2) of sequential reactions are of the same magnitude, the data are equally well described using rate laws where $k_1 < k_2$ and $k_1 > k_2$. However, in the present case, we have independently measured the rates of oxidation of PhSO_2^- by HOCl (Figure 7, top) and the rates of hydrolysis of PhSO_2Cl (Figure 4). Accordingly, we are able to attribute the data of Figure 7 (bottom) to the oxidation and hydrolysis steps (Table 3). Note that the oxidation step of Figure 7 (top) and Table 3 (last two columns) exhibit an inverse dependency on $[\text{OH}^-]$ (as expected for reaction by HOCl), whereas the rate of

hydrolysis is proportional to $[\text{OH}^-]$. Importantly, since the rate constant for the reaction of HOCl with PhSO_2^- (k_{HOCl}) must be extrapolated by 5.6–6.6 orders of magnitude to the $\text{p}K_a$ of HOCl, the data of Figure 7 are not necessarily expected to yield a precise value for k_{HOCl} . However, the actual objective of collecting the data of Figure 7 was to determine the value of the rate constant for the reaction of OCl^- with PhSO_2^- (k_{OCl} , the rate constant that Kice and Puls thought they were measuring), which is contained in the intercept of the line of the inset of Figure 7. The values of k_{HOCl} and k_{OCl} will be evaluated when the rate law is derived in the Discussion.

Discussion

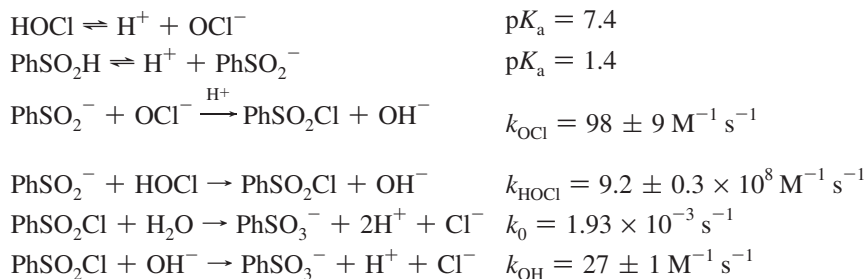
Mechanism of the Hydrolysis of ArSO_2Cl . The kinetics and mechanism of the hydrolysis of aliphatic and aromatic sulfonyl chlorides have been previously investigated in detail.^{11,12} Our objectives here were simply to establish whether TNBO_2Cl behaves as a typical aryl sulfonyl chloride and (in the case of PhSO_2Cl) to extend the range of reaction conditions to include the conditions we employed in our kinetic studies of the oxidation reaction (namely to employ $I = 1.0$ and to extend the pH above pH 11). The rate of hydrolysis of ArSO_2Cl can be described by the following rate law:

$$-\text{d}[\text{ArSO}_2\text{Cl}]/\text{d}t = k_{\text{obs}}[\text{ArSO}_2\text{Cl}] = (k_0 + k_{\text{OH}}[\text{OH}^-])[\text{ArSO}_2\text{Cl}] \quad (1)$$

We have interpreted the rate law as hydrolysis by H_2O (k_0) and by OH^- (k_{OH}). The data we have measured for TNBO_2Cl are described by eq 1. While we did not reinvestigate the rate of hydrolysis of PhSO_2Cl below pH 13, our value of $k_{\text{OH}} = 27 \pm 1 \text{ M}^{-1} \text{ s}^{-1}$ for $I = 1$ (Figure 4) is comparable to the value of $k_{\text{OH}} = 28.2 \text{ M}^{-1} \text{ s}^{-1}$ that has been reported previously for pH < 11 and $I = 50 \text{ mM}$.¹¹

Mechanism of the Reaction of PhSO_2^- with HOCl/ OCl^- . We conclude that the mechanism of Scheme 1 is operative because (1) the reaction of PhSO_2^- with HOCl/ OCl^- quantitatively yields PhSO_2Cl at pH < 8, conditions under which hydrolysis is relatively slow (cf. Figure 1); (2) PhSO_2Cl is produced as a transient under conditions where the rate of hydrolysis is competitive with rate of oxidation (Figure 7); and (3) the rate of oxidation of PhSO_2^- by HOCl/ OCl^- exhibits an inverse dependence on $[\text{OH}^-]$, even under very alkaline conditions (Figure 7, inset). Assuming that the Brønsted acid/base reaction is fast (diffusion-controlled), the following rate law is readily derived (for pH ≥ 9 , where OCl^- dominates over HOCl):

SCHEME 1: Kinetics and Mechanism of the Oxidation of PhSO_2^- with HOCl/ OCl^-



$$\text{Rate} = \frac{-\text{d}[\text{PhSO}_2^-]}{\text{d}t} = \frac{-\text{d}[\text{OCl}^-]}{\text{d}t} = \left(\frac{k_{\text{OCl}} \cdot K_a^{\text{HOCl}} + k_{\text{HOCl}} \cdot [\text{H}^+]}{K_a^{\text{HOCl}} + [\text{H}^+]} \right) \cdot [\text{HOCl}]_{\text{T}} \cdot [\text{PhSO}_2^-] \quad (2)$$

where $[\text{HOCl}]_{\text{T}} = [\text{HOCl}] + [\text{OCl}^-] \approx [\text{OCl}^-]$ (for pH > 9). For the data of Figure 6, the second term of the numerator dominates and $K_a^{\text{HOCl}} \gg [\text{H}^+]$, so eq 2 simplifies to give the observed pseudo-second-order rate constant:

$$k_{\text{obs}} = \frac{k_{\text{HOCl}} \cdot [\text{H}^+]}{K_a^{\text{HOCl}}} \quad (3)$$

Solving for k_{HOCl} and inserting $[\text{H}^+] = 10^{-9} \text{ M}$ and $K_a^{\text{HOCl}} = 10^{-7.4} \text{ M}$ gives a value of

$$k_{\text{HOCl}} = \frac{k_{\text{obs}} \cdot K_a^{\text{HOCl}}}{[\text{H}^+]} = \frac{2.32 \times 10^7 \text{ M}^{-1} \text{ s}^{-1} \cdot 10^{-7.4} \text{ M}}{10^{-9} \text{ M}} = 9.2 \pm 0.3 \times 10^8 \text{ M}^{-1} \text{ s}^{-1} \quad (4)$$

The value for k_{HOCl} from eq 4 is consistent with values we have determined by SVD analysis of data at higher pH (Table 2, $\bar{X} = (2.4 \pm 0.8) \times 10^8 \text{ M}^{-1} \text{ s}^{-1}$), where the rate of hydrolysis is competitive with the rate of oxidation. Thus, k_{HOCl} is very close to the diffusion limit. It is also possible to extrapolate a value of k_{HOCl} using the data of Figure 7. The linear fit of the data of Figure 7 (inset) suggests that k_{HOCl} still influences the rate above pH 13. Applying eq 3 to the slope of the line, multiplying by $[\text{OH}^-]$ (because plot is $1/[\text{OH}^-]$ vs k_{obs}), multiplying by $[\text{HOCl}]_0 = 1 \text{ mM}$ (pseudo-first-order-conditions), and solving for k_{HOCl} (while substituting $K_w = [\text{H}^+][\text{OH}^-] = 10^{-13.8} \text{ M}^2$)¹³ gives

$$k_{\text{HOCl}} = \frac{\text{slope} \cdot K_a^{\text{HOCl}}}{K_w \cdot [\text{HOCl}]_0} = \frac{0.1034 \pm 0.003 \text{ M}^{-1} \text{ s}^{-1} \cdot 10^{-7.4} \text{ M}}{(10^{-13.8} \text{ M}) \cdot (0.001 \text{ M})} = 3.3 \pm 0.1 \times 10^8 \text{ M}^{-1} \text{ s}^{-1} \quad (5)$$

The values of k_{HOCl} that were determined from the data of Figure 6, Table 2, and Figure 7 (inset) are self-consistent (within a factor of 4 over a $\Delta[\text{H}^+]$ of 4 orders of magnitude). In addition, the intercept of the line of Figure 7 (inset, which is proportional to k_{OCl}) appears to be significant; we estimate k_{OCl} to be 98

$9 \text{ M}^{-1} \text{ s}^{-1}$. Therefore, about a 7 orders of magnitude difference exists between k_{HOCl} and k_{OCl^-} , and 6.6 decades of difference exists between the $\text{p}K_{\text{a}}$ of HOCl (OCl^- would be protonated below pH 7.4 and the rate of HOCl would reach a maximum) and pH 13. Thus, at about pH 13, the reaction of OCl^- is competitive with the reaction of HOCl. Scheme 1 summarizes the acid dissociation of HOCl⁷ and PhSO_2H ,¹⁴ the rate data we report for the oxidation of PhSO_2^- with HOCl/ OCl^- (using the value of k_{HOCl} that was measured at the lowest possible pH) and the subsequent hydrolysis of PhSO_2Cl (the value of k_0 in Scheme 1 is from the literature).¹¹

Previous Mechanistic Studies. Besides the work of Kice and Puls that has been the subject of the present paper,⁵ there have been few previous mechanistic studies of the oxidation of sulfonates.¹⁵ It has been previously suggested that the oxidation of cysteine by ClO_2 under acidic condition involves a cysteinyl- ClO_2 adduct that subsequently hydrolyzes to give cysteine sulfinic acid and HOCl in a rate-limiting step, with subsequent oxidation of the sulfinate by HOCl to give cysteine sulfonate.¹⁶ However, the kinetics of the reaction of cysteine sulfinate with HOCl to give the sulfonate were not investigated. The rate constants for the reactions of ArSO_2^- with HOCl of ca. 10^9 that have been reported herein are unexpectedly large. Given the electrophilic nature of HOCl, it follows that the best nucleophiles should be the most reactive. This is the case for the amino acids, where the most nucleophilic sulfur donors cysteine and methionine are most reactive.³ A similar situation is found for inorganic ions.¹⁷ Given the fact that sulfonates are considerably less nucleophilic than thiolates,¹⁸ it is surprising that ArSO_2^- reacts with HOCl with rate constants that are several orders of magnitude larger than those for thiolates.³

As an aside, it has recently become appreciated that sulfinic acid modifications in proteins link protein function to cellular oxidative status,¹⁹ and that HOCl is produced by the oxidation of Cl^- with H_2O_2 in a reaction that is catalyzed by human neutrophilic myeloperoxidase.²⁰ Accordingly, we are particularly interested in the possible role of the oxidation of sulfonates by HOCl in the context of biomarkers²¹ for myeloperoxidase-induced oxidative stress (that may be linked to inflammatory diseases²²). While we had previously thought it was improbable that sulfonates could compete kinetically with typical antioxidants in vivo (such as the ubiquitous thiol-containing tripeptide glutathione) the results of the present study have caused us to reconsider that position.

Conclusions

The oxidation of ArSO_2^- (PhSO_2^- and TNBO_2^{2-}) with HOCl/ OCl^- proceeds via a conventional pathway: nucleophilic attack by ArSO_2^- on HOCl with concomitant Cl^+ transfer to give a sulfonyl chloride intermediate (ArSO_2Cl), which we have identified spectrophotometrically. Remarkably, the rate constant for the reaction of HOCl with ArSO_2^- is on the order of 10^9

$\text{M}^{-1} \text{ s}^{-1}$, similar to that of the corresponding thiolates, and nearly diffusion-controlled. In contrast, the rate constant for the reaction of OCl^- with ArSO_2^- is approximately 7 orders of magnitude smaller.

Acknowledgment. This research was funded by the National Science Foundation (CHE-0503984).

Supporting Information Available: UV-vis spectra of PhSO_2^- , PhSO_3^- , PhSO_2Cl , TNBO_2^{2-} , TNBO_3^{2-} , and TNBO_2Cl . This material is available free of charge via the Internet at <http://pubs.acs.org>.

References and Notes

- (1) References to compounds without charges are inclusive of all acid/base derivatives (e.g., TNB). Reference to specific proton states are indicated with a charge (e.g., TNB0, TNB^- , and TNB^{2-}).
- (2) Nagy, P.; Ashby, M. T. *J. Am. Chem. Soc.* **2007**, *129*, 14082.
- (3) Gerritsen, C. M.; Margerum, D. W. *Inorg. Chem.* **1990**, *29*, 2757.
- (4) Fogelman, K. D.; Walker, D. M.; Margerum, D. W. *Inorg. Chem.* **1989**, *28*, 986.
- (5) Kumar, K.; Margerum, D. W. *Inorg. Chem.* **1987**, *26*, 2706.
- (6) Pattison, D. I.; Davies, M. J. *Chem. Res. Toxicol.* **2001**, *14*, 1453.
- (7) Nagy, P.; Ashby, M. T. *Chem. Res. Toxicol.* **2005**, *18*, 919.
- (8) Nagy, P.; Ashby, M. T. *Chem. Res. Toxicol.* **2007**, *20*, 79.
- (9) Kice, J. L.; Puls, A. R. *J. Am. Chem. Soc.* **1977**, *99*, 3455.
- (10) Landino, L. M.; Mall, C. B.; Nicklay, J. J.; Dutcher, S. K.; Moynihan, K. L. *Nitric Oxide* **2008**, *18*, 11.
- (11) Adam, L. C.; Fabian, I.; Suzuki, K.; Gordon, G. *Inorg. Chem.* **1992**, *31*, 3534.
- (12) Wang, T. X.; Margerum, D. W. *Inorg. Chem.* **1994**, *33*, 1050.
- (13) Eigen, M.; Kustin, K. *J. Am. Chem. Soc.* **1962**, *84*, 1355.
- (14) Lifshitz, A.; Perlmutter-Hayman, B. *J. Phys. Chem.* **1962**, *66*, 701.
- (15) Tomomura, B.; Nakatani, H.; Ohnishi, M.; Yamaguchi-Ito, J.; Hiromi, K. *Anal. Biochem.* **1978**, *84*, 370.
- (16) Dunn, B. C.; Meagher, N. E.; Rorabacher, D. B. *J. Phys. Chem.* **1996**, *100*, 16925.
- (17) Rogne, O. *J. Chem. Soc. B* **1968**, 1294.
- (18) Kevill, D. N.; Park, B.-C.; Park, K.-H.; D'Souza, M. J.; Yaakoub, L.; Mlynarski, S. L.; Kyong, J. B. *Org. Biomol. Chem.* **2006**, *4*, 1580.
- (19) Koo, I. S.; Yang, K.; Park, J. K.; Woo, M. Y.; Cho, J. M.; Lee, J. P.; Lee, I. *Bull. Korean Chem. Soc.* **2005**, *26*, 1241.
- (20) Koo, I. S.; Yang, K.; Shin, H. B.; An, S. K.; Lee, J. P.; Lee, I. *Bull. Korean Chem. Soc.* **2004**, *25*, 699.
- (21) Ivanov, S. N.; Kislov, V. V.; Gnedin, B. G. *Russ. J. Gen. Chem.* **2004**, *74*, 95.
- (22) Martell, A. E.; Smith, R. M. *Inorganic Complexes*; Critical Stability Constants, Vol. 4; Plenum Press: New York, 1976.
- (23) Ogata, Y.; Sawaki, Y.; Isono, M. *Tetrahedron* **1970**, *26*, 3045.
- (24) Gancarz, R. A.; Kice, J. L. *Tetrahedron Lett.* **1980**, *21*, 1697.
- (25) Ison, A.; Odeh, I. N.; Margerum, D. W. *Inorg. Chem.* **2006**, *45*, 8768.
- (26) Nagy, P.; Lemma, K.; Ashby, M. T. *Inorg. Chem.* **2007**, *46*, 285.
- (27) Ritchie, C. D.; Virtanen, P. O. I. *J. Am. Chem. Soc.* **1972**, *94*, 4966.
- (28) Ritchie, C. D.; Saltiel, J. D.; Lewis, E. S. *J. Am. Chem. Soc.* **1961**, *83*, 4601.
- (29) Okuyama, T. In *The Chemistry of Sulphinic Acids, Esters, and Their Derivatives*; Patai, S., Ed.; John Wiley & Sons: New York, 1990; p 639.
- (30) Jacob, C.; Holme, A. L.; Fry, F. H. *Org. Biomol. Chem.* **2004**, *2*, 1953.
- (31) Klebanoff, S. J. *J. Leukocyte Biol.* **2005**, *77*, 598.
- (32) Harwood, D. T.; Nimmo, S. L.; Kettle, A. J.; Winterbourn, C. C.; Ashby, M. T. *Chem. Res. Toxicol.* **2008**, *21*, 1011.
- (33) Ashby, M. T. *J. Dent. Res.* **2008**, *87*, 900.
- (34) Pattison, D. I.; Davies, M. J. *Curr. Med. Chem.* **2006**, *13*, 3271.

JP906651N